Inorganic Chemistry

Article

pubs.acs.org/IC

One-Pot Noninjection Synthesis of Cu-Doped $Zn_xCd_{1-x}S$ Nanocrystals with Emission Color Tunable over Entire Visible Spectrum

Wenjin Zhang, Xinggui Zhou, and Xinhua Zhong*

State Key Laboratory of Chemical Engineering, Department of Chemistry, East China University of Science and Technology, Shanghai 200237, China

Supporting Information

ABSTRACT: Unlike Mn doped quantum dots (d-dots), the emission color of Cu dopant in Cu d-dots is dependent on the nature, size, and composition of host nanocrystals (NCs). The tunable Cu dopant emission has been achieved via tuning the particle size of host NCs in previous reports. In this paper, for the first time we doped Cu impurity in $Zn_xCd_{1-x}S$ alloyed NCs and tuned the dopant emission in the whole visible spectrum via variation of the stoichiometric ratio of Zn/Cd precursors in the host $Zn_xCd_{1-x}S$ alloyed NCs. A facile noninjection and low cost approach for the synthesis of Cu:$Zn_xCd_{1-x}S$ d-dots was reported. The optical properties and structure of the obtained Cu:$Zn_xCd_{1-x}S$ d-dots have been characterized by UV−vis spectroscopy, photoluminescence (PL) spectroscopy, transmission electron microscopy (TEM), and X-ray diffraction (XRD). The influences of various experimental variables, including Zn/Cd ratio, reaction temperature, and Cu dopant concentration, on the optical properties of Cu dopant emission have been systematically investigated. The as-prepared Cu:$Zn_xCd_{1-x}S$ d-dots did show PL emission but with quite low quantum yield (QY) (typically below 6%). With the deposition of ZnS shell around the Cu:$Zn_xCd_{1-x}S$ core NCs, the PL QY increased substantially with a maximum value of 65%. More importantly, the high PL QY can be preserved when the initial oil-soluble d-dots were transferred into aqueous media via ligand replacement by mercaptoundeconic acid. In addition, these d-dots have thermal stability up to 250 °C.

INTRODUCTION

Luminescent colloidal semiconductor nanocrystals (NCs) or quantum dots (QDs) have been extensively explored as an attractive alternative to organic dyes for applications in the fields of display or lighting devices,[1−3] photovoltaics,[4−6] and biomedical labeling or diagnostics[7−9] during the past two decades due to their unique size and composition tunable band edge photoluminescence (PL). In recent developments, doped semiconductor quantum dots (d-dots) are increasingly being investigated since they can not only retain nearly all intrinsic advantages of QDs but also possess additional advantages such as larger Stokes shift to avoid self-absorption/energy transfer, enhanced thermal and chemical stability, and longer excited state lifetime.[10−12] Along this direction, Cu- and Mn-doped zinc chalcogenide d-dots were demonstrated as efficient emitters covering the blue to orange color window.[13−47] For Mn d-dots, the dopant emission is considered to come from $Mn^{2+4}T_1-{}^6A_1$ transition. This leads to such emission which is relatively independent of the nature and size of host NCs, and thus, Mn dopant emission is restricted within the yellow-orange spectral window (580−600 nm).[13−36] However, for many applications, an emission wavelength range that is as wide as possible is preferred. The Cu d-dots have the potential to support a wide range of emission wavelength since in this system the excitons of the host NCs relax through the recombination of the electron in the conduction band of host material and hole in Cu T_2 state.[48] Therefore, Cu d-dots could be a potentially color tunable NC emitter with emission color spanning over a wide spectral range dependent on the nature, size, and composition of host NCs.[37−47] In previous reports, the Cu dopant emission in ZnS host NCs shows blue-green emission;[40,47] in ZnSe, it is a little more extended to greenish yellow spectral window;[43,46,47] in CdS, it is is orange-red;[48c,d] in InP, it has been extended to near IR;[42] in Zn−In−Se, it shows emission over most of the visible window;[45] and recently in $ZnS/Zn_xCd_{1-x}S$ surface alloyed NCs it covers the blue to red end of the visible spectrum.[44] It should be noted that, in ref 44, the authors had tried to dope Cu in the Zn−Cd−S alloyed NCs, but failed to achieve significant dopant emission.

Herein, we reported a facile one-pot noninjection synthesis of Cu:$Zn_xCd_{1-x}S$ d-dots with all reactants loaded in the reaction flask at room temperature. After overcoating ZnS shell around the Cu:$Zn_xCd_{1-x}S$ cores directly in the crude reaction solution, the resultant Cu:$Zn_xCd_{1-x}S$/ZnS d-dots show composition-tunable emission over the entire visible spectral window (from 440 to 710 nm) with highest PL quantum yield (QY) up to 65%. Importantly, the initial high PL QY of the obtained Cu:$Zn_xCd_{1-x}S$/ZnS d-dots in organic media can be preserved when transferred into aqueous media via ligand exchange by hydrophilic ligands. The obtained Cu:$Zn_xCd_{1-x}S$/ZnS d-dots with an intense, thermally stable, wide range of tunable dopant

Received: November 7, 2011
Published: February 24, 2012

   dx.doi.org/10.1021/ic2024023 | Inorg. Chem. 2012, 51, 3579−3587

emission could be a promising candidate for applications ranging from optoelectronics to biomedical labeling. Furthermore, this facile noninjection synthetic strategy provides a versatile route for a scalable, reproducible, and low cost preparation of other doped semiconductor NCs for potential industrial applications.

EXPERIMENTAL SECTION

Chemicals. Zinc acetate ($Zn(OAc)_2$, 99.99%), cadmium oxide (CdO, 99.99+%), copper acetate ($Cu(OAc)_2$, 99.99%), sulfur powder (99.99%), dodecanethiol (DDT, 99.9%), oleic acid (OA, 90%), oleylamine (OAm, 97%), 1-octadecene (ODE, 90%), 11-mercaptoundecanoic acid (MUA, 95%), and tetramethylammonium hydroxide (TMAH, 97%) were purchased from Aldrich. All chemicals were used without further purification.

Preparation of Stock Solutions. Zn stock solution (0.1 M) was obtained by dissolving 0.440 g (2 mmol) of $Zn(OAc)_2$ in 1.6 mL of OAm, and 18.4 mL of ODE at 160 °C under nitrogen flow. Cd stock solution (0.1 M) was obtained by dissolving 0.256 g (2 mmol) of CdO in 4.0 mL of OA, and 16.0 mL of ODE at 160 °C under nitrogen flow. Cu stock solution (0.01 M) was obtained by dissolving 0.010 g (0.05 mmol) of $Cu(OAc)_2$ in 0.2 mL of OAm, and 4.8 mL of ODE at 90 °C under nitrogen flow. Zn stock solution (0.4 M) for ZnS shell was obtained by dissolving 1.756 g (8 mmol) of $Zn(OAc)_2$ in 6.0 mL of OAm, and 14.0 mL of ODE at 160 °C under nitrogen flow. All the prepared stock solutions were stored at 50 °C for uses to follow.

Synthesis of Cu:$Zn_xCd_{1-x}S$ and Cu:$Zn_xCd_{1-x}S$/ZnS d-Dots. In a typical procedure, 1.0 mL of Zn stock solution (0.1 mmol), 1.0 mL of Cd stock solution (0.1 mmol), 0.2 mL of Cu stock solution (0.002 mmol), 1.0 mL of ODE-S solution (0.4 mmol), obtained by dissolving 4.0 mmol of sulfur in 10.0 mL of ODE at 120 °C, 1.0 mL of DDT, and 2.0 mL of ODE were loaded in a 50-mL three-neck flask clamped in a heating mantle. The mixture was heated to 220 °C from room temperature with a rate of 15 °C/min under argon flow and kept at this temperature to allow growth of Cu:$Zn_xCd_{1-x}S$ d-dots. Aliquots of the sample were taken at different time intervals and injected into cold toluene to terminate growth of d-dots immediately to use for recording their optical spectra. After completion of particle growth, the reaction mixture was cooled to 60 °C, and 10 mL of toluene was added thereafter. The obtained Cu:$Zn_xCd_{1-x}S$ d-dots were precipitated by adding methanol into the toluene solution and purified by repeated centrifugation and decantation. For obtaining Cu:$Zn_xCd_{1-x}S$ d-dots with different Zn/Cd ratios, the Zn/Cd precursor ratio was varied while other variables were kept constant.

Deposition of ZnS shell around the Cu:$Zn_xCd_{1-x}S$ core template was carried out in the crude Cu:$Zn_xCd_{1-x}S$ reaction mixture after growth time of 30 min. The overcoating procedure was performed at the same temperature as core growth. The entire stock solution of Zn precursor (3.0 mL) was injected into the reaction system in 0.5 mL portion at intervals of 15 min. As part of monitoring the reaction, aliquots were taken before the injection of a new portion of Zn stock solution, and their corresponding optical spectra were recorded accordingly. Purification of Cu:$Zn_xCd_{1-x}S$/ZnS d-dots was similar to that of Cu:$Zn_xCd_{1-x}S$ d-dots.

Water Solubilization of Oil-Soluble Cu:$Zn_xCd_{1-x}S$/ZnS d-Dots via Ligand Exchange. Water solubilization of the initially oil-soluble Cu:$Zn_xCd_{1-x}S$/ZnS d-dots was achieved by replacing the initial hydrophobic surfactants with thiol-containing hydrophilic ligand (MUA) according to the literature method.[49] Typically, MUA (0.5 g) was dissolved in 5.0 mL of methanol, and the pH of the solution was adjusted to 9 with addition of TMAH. The MUA methanol solution (0.5 mL) was then added to 5.0 mL of purified Cu:$Zn_xCd_{1-x}S$/ZnS d-dots chloroform solution (with absorbance of 0.5) and stirred vigorously for 30 min at 70 °C to get precipitation of NCs. Then, 5.0 mL of distilled water was added into the mixture and kept stirring for another 20 min. The solution was separated into two phases finally, and the NCs were transferred into the supernatant aqueous phase from the underlying toluene, which was discarded, and the aqueous phase containing the NCs was collected. The free MUA in NCs aqueous solution was isolated by precipitating the NCs with addition of acetone. The supernatant was discarded, and the pellet was then redissolved in water to get the purified NC aqueous solution for further use.

Characterization. UV–vis and PL spectra were obtained on a Shimadzu UV-2450 UV–vis spectrophotometer and a Cary Eclipse (Varian) fluorescence spectrophotometer, respectively. The room-temperature PL QYs of NCs were determined by comparing the integrated emission of the NCs samples in solution with that of a fluorescent dye (rhodamine 6G in ethanol or rhodamine 101 in 0.01% HCl ethanol solution) with identical optical density.[50,51] Also, the known QYs of the NCs in solution can be used to measure the PL efficiencies of other NCs by comparing their integrated emission. The fluorescence lifetime study was performed by an Edinburgh FL 900 single-photon counting system equipped with a Hamamatsu C8898 ps light pulser. The excitation light was obtained from a 441 nm laser light. The luminescence time range was selected at 0–200 ns. Data were analyzed using a nonlinear least-squares fitting program, with deconvolution of the exciting pulse being ~200 ps. Transmission electron microscopy (TEM) images were acquired using a JEOL JEM-1400 transmission electron microscope operating at an acceleration voltage of 120 kV. The TEM samples were prepared by depositing a drop of dilute NC toluene solutions onto copper grids with carbon support. Powder X-ray diffraction (XRD) was obtained by wide-angle X-ray scattering using a Siemens D5005 X-ray powder diffractometer equipped with graphite-monochromatized Cu Kα radiation (λ = 1.5406 Å). XRD samples were prepared by depositing NC powder on a piece of Si(100) wafer. The composition for the NCs was measured by means of inductively coupled plasma atomic emission spectroscopy (ICP-AES, Thermo Elemental IRIS 1000) using HCl/HNO_3 digestion.

RESULT AND DISCUSSION

Synthesis and Optical Properties of Cu:$Zn_xCd_{1-x}S$ d-dots. Herein, we chose $Zn_xCd_{1-x}S$ alloyed NCs as the host material for prepared Cu d-dots. It is noted that Pradhan and co-workers had tried to dope $Zn_xCd_{1-x}S$ alloyed NCs with Cu impurity, but failed to achieve significant dopant emission.[44] The same group then designed cubic ZnS NC seeds to adsorb the Cu dopant ions, and the Zn–Cd–S alloyed NCs shell was further grown to bury the adsorbed dopant ions. Intense and tunable emission of Cu dopant was observed in the resulting Cu doped ZnS/$Zn_xCd_{1-x}S$ surface alloyed NCs. Our synthetic strategy for Cu:$Zn_xCd_{1-x}S$ d-dots is based on a nucleation doping technique where the precursors for dopant and host material are loaded together at room temperature and a minimum amount of dopant is then introduced in the host NCs during nucleation and growth stage at high temperature. In the synthetic experiments, all precursors ($Cu(OAc)_2$, CdO, $Zn(OAc)_2$, and S) along with the capping agent DDT and solvent ODE were loaded together in a reaction flask at room temperature and then heated to 220 °C under nitrogen flow. Within about 30 min, the Cu dopant emission evolved and intensified with the reaction time and the highest PL QY could reach about 6%. Further injection of Zn precursor to the preformed Cu:$Zn_xCd_{1-x}S$ d-dots system with the presence of excess sulfur precursor led to the formation of Cu:$Zn_xCd_{1-x}S$/ZnS core/shell nanostructure, and the corresponding PL QY was enhanced to more than 50%. The compound of DDT serves as sulfur source and stabilizing ligand for the formed NCs simultaneously. It was noted that thiols are soft Lewis base ligands for transition metal ions and thus can form stable metal complexes to lower the reactivity of metal ion precursors. In previous reports, thiols were successfully used as ligands for formation of high-quality I–III–VI semiconductor NCs by balancing the reactivity of evolved cationic precursors.[49,52,53]

dx.doi.org/10.1021/ic2024023 | Inorg. Chem. 2012, 51, 3579–3587

With prolonging reaction time, solution color turned slowly from light yellow to yellow, which indicated the start of nucleation and the following NC growth. The temporal evolution of the absorption and emission spectra of Cu:$Zn_xCd_{1-x}S$ d-dots prepared under initial Zn/Cd/Cu precursor ratio of 50:50:1 in ODE media at growth temperature of 220 °C was shown in Figure 1. The observed non-

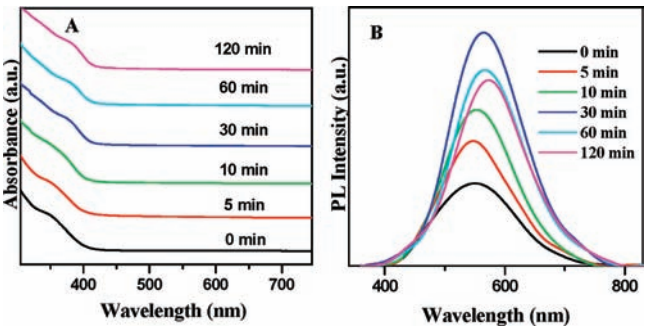

Figure 1. Temporal evolution of (A) UV–vis absorption and (B, λ_{ex} = 350 nm) PL emission spectra of Cu:$Zn_xCd_{1-x}S$ d-dots dispersed in chloroform solution.

distinguished broad peak in the absorption spectra (Figure 1A) is assigned to the excitonic transition of the $Zn_xCd_{1-x}S$ host alloyed NCs, which underwent a small red-shift from 360 to 376 nm, but spectral shape kept almost no variation during a period of 2 h growth time. This poorly resolved excitonic absorption peak is characteristic of ternary and quaternary alloyed NCs, which is not caused solely by the wide size distribution since the special electronic properties are considered as one possible reason, and the irregular composition distribution among different NCs in an ensemble can also be one of the reasons.[54] Figure 1B shows that the corresponding PL peak position red-shifted monotonously from 550 to 575 nm with prolonging reaction time, and the highest PL intensity was observed with annealing time of 30 min. With a further extension of the heating time, the PL intensity decreased gradually.

Structural characterization for the obtained Cu:$Zn_xCd_{1-x}S$ d-dots was carried out by means of TEM and XRD. Figure 2 shows the TEM images and XRD patterns of the representative d-dots samples with growth time of 30 min at 220 °C. The TEM images demonstrate that all of the as-obtained NCs are of near-spherical shape and possess high size uniformity. The average diameter of the d-dots was determined to be 3.2 ± 0.3 nm, and the corresponding histograms of size distribution are shown in the inset. The wide-angle XRD patterns of the obtained d-dots displayed the characteristic peaks of the zinc blende (cubic) structure, which were located between those for cubic ZnS and CdS materials. This feature confirms the $Zn_xCd_{1-x}S$ alloy structure. As per the reported failure of Cu doping in the wurtzite Zn–Cd–S alloyed host,[44] our observed zinc blende crystalline phase of the host $Zn_xCd_{1-x}S$ NCs supports the hypothesis that Cu ions are easier to incorporate into zinc blende host NCs than in wurtzite and rock-salt crystals.[12] No diffraction peaks from Cu impurities were detected in the samples. In addition, we can conclude that doping Cu into the host alloyed NCs does not bring about a phase transformation of the crystal structure.

Host NCs Composition-Tuned Dopant Emission. The most acceptable explanation supposes that Cu dopant emission

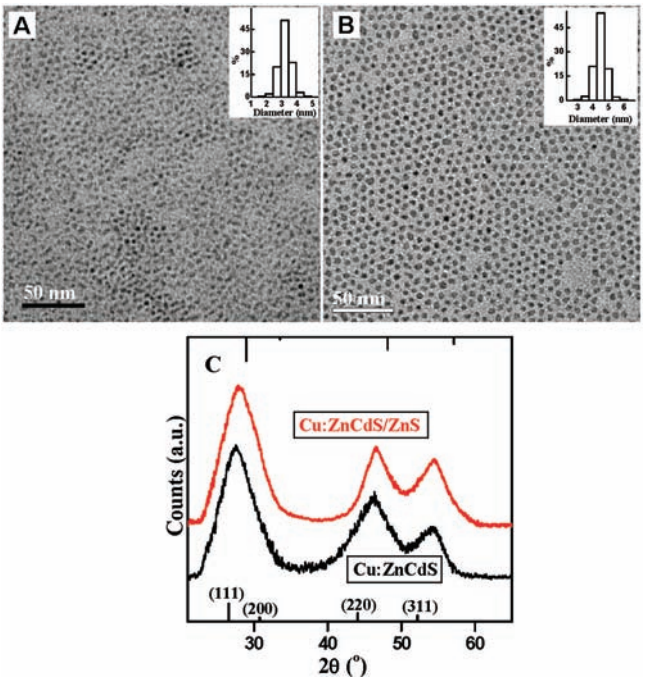

Figure 2. Wide-filed TEM images of (A) Cu:$Zn_xCd_{1-x}S$ d-dots sample with growth time of 30 min, and (B) the derivate Cu:$Zn_xCd_{1-x}S$/ZnS d-dots. Insets are the corresponding histograms of the size distribution. (C) XRD patterns of the samples as shown in parts A and B. The line XRD spectra correspond to bulk (bottom) zinc blende CdS and (top) zinc blende ZnS.

in d-dots is derived from the recombination of the electron in the conduction band of host material and hole in Cu T_2 state, which stays above the valence band of semiconductor host, and after excitation the valence hole transfers to this T_2 state.[48] Therefore, Cu d-dots could be a potential color tunable NC emitter with emission color dependent on the nature, size, and composition of host NCs. As reported in previous literature, tuning Cu dopant emission can be achieved by varying particle size of the host binary semiconductor NCs ZnS, ZnSe, and InP, etc.[40,42,43,46,47] Besides the particle size in binary semiconductor NCs, the composition in ternary alloyed NCs can also serve as a possible alternative to tune the conduction edge of the host material in Cu d-dots and accordingly tunes the Cu dopant emission color. Ternary $Zn_xCd_{1-x}S$ alloyed NCs are promising host materials for Cu d-dots due to their ideal band edge absorption to achieve wide tunable dopant emission.

In our synthesis of Cu:$Zn_xCd_{1-x}S$ d-dots, the composition of the host $Zn_xCd_{1-x}S$ alloyed NCs was tuned via the variation of Zn/Cd precursor ratio in the synthetic step. In the experiments, the molar ratio of Cd/Zn precursors was varied from 0.25:1 to 16:1 with fixation of the gross amount of Cd and Zn precursors at 0.2 mmol. It should be noted that no PL was observed in the resulting Cu:$Zn_xCd_{1-x}S$ d-dots when the Cd/Zn ratio was less than 0.25:1; thus, no results corresponding to samples with Cd/Zn ratio less than 0.25 were reported. With ICP-AES measurement the amounts of Zn and Cd in the obtained Cu:$Zn_xCd_{1-x}S$ samples were determined. From these results the Cd/Zn atomic ratios were calculated and compared with the nominal values. The nominal Cd/Zn ratios used in the synthesis and the real Cd/Zn ratios in samples determined by ICP-AES are given in Table 1. It can be found that the real Cd/Zn ratio in actual samples is higher than the nominal value.

dx.doi.org/10.1021/ic2024023 | Inorg. Chem. 2012, 51, 3579–3587

Table 1. Nominal Zn/Cd Atomic Ratios Used in the Synthesis and the Real Zn/Cd Atomic Ratios in Cu:$Zn_xCd_{1-x}S$ d-Dot Samples Determined by ICP-AES

nominal Cd/Zn atomic ratio	ICP results of Cd/Zn ratio in Cu:$Zn_xCd_{1-x}S$ samples
0.25:1	0.29:1
1:1	1.2:1
2:1	2.3:1
4:1	4.6:1
8:1	9.1:1
16:1	18.3:1

This indicates the less activity of Zn precursor compared with that of Cd precursor and the phenomena has been observed in the synthesis of $Zn_xCd_{1-x}S$ alloy NCs in previous literature reports.[51,55]

Experimental results show that, with the increase of nominal Cd/Zn precursor ratio from 0.25:1 to 16:1, the first excitonic absorption peak of the intrinsic $Zn_xCd_{1-x}S$ alloyed NCs became much more pronounced and red-shifted systematically from 327 to 440 nm (Figure 3A). As expected, accompanied with the red shift of excitonic absorption peak, the corresponding Cu dopant emission red-shifted also, but at a much more pronounced extent from 450 to 710 nm (Figure 3B). It is noted that, with the increase of Cd/Zn precursor ratio in the preparation of Cu:$Zn_xCd_{1-x}S$ d-dots, the particle size remained almost constant (corresponding TEM images available in Figure S1 of Supporting Information, SI). The features of fixation of particle size combining the red-shift of excitonic absorption peak give strong evidence to confirm the alloy structure of the host Zn−Cd−S NCs. Figure 3C summarizes the dependence of PL intensity and PL peak position of the dopant emission in the resulting Cu:$Zn_xCd_{1-x}S$ d-dots on the Cd/Zn ratio of the samples. In principle, with increase of Cd/Zn ratio from 0.29:1 to 18.3:1, the PL intensity increased rapidly and approached the highest intensity (with ~6% PL QY) at Cd/Zn ratio of 1.2:1. With further increase of the Cd/Zn ratio, the PL emission reduced systematically. The deep red emission from the obtained Cu:$Zn_xCd_{1-x}S$ samples can rule out the band edge emission from host $Zn_xCd_{1-x}S$ NCs, since the bulk band gap of CdS and ZnS are 2.5 eV (506 nm) and 3.7 eV (335 nm), respectively. As for the explanation of the observed remarkable red-shift (from 450 to 710 nm) of Cu dopant emission with the increase of Cd/Zn ratio, it is well-known that, with the increase of content of low band gap CdS in the $Zn_xCd_{1-x}S$ alloyed NCs, the band gap of the alloyed NCs decreases accordingly. Because of the much smaller electron effective mass versus the significantly larger hole mass, most of the band gap decrease is seen as a shift in the conduction band to lesser negative potentials;[56] thus, it results in lowering down of the Cu dopant emission, which is derived from the recombination of the electron in the conduction band of host material and hole in Cu T_2 state.

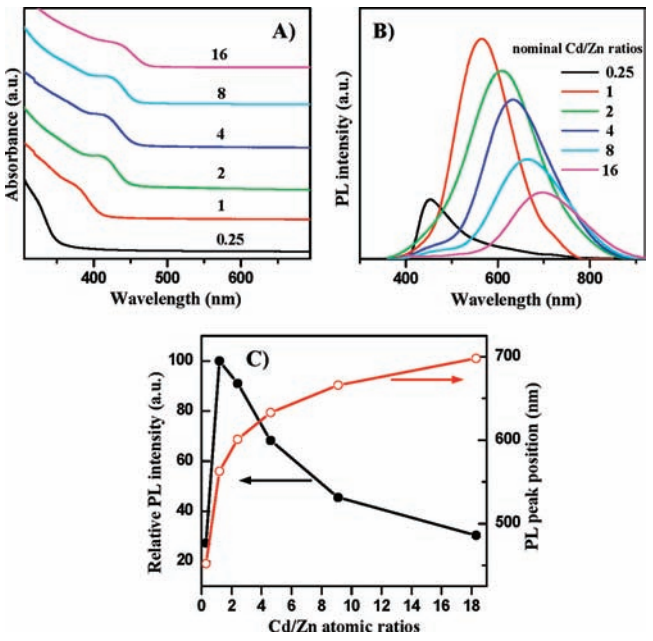

Figure 3. (A) Absorption and (B, λ_{ex} = 350 nm) PL emission spectra of Cu:$Zn_xCd_{1-x}S$ d-dots under different Cd/Zn precursor ratios. (C) Summarization of the dependence of relative PL intensity and peak position of the Cu:$Zn_xCd_{1-x}S$ d-dots on the Cd/Zn ratio in the samples.

Lifetime of PL. Even though the deep red PL emission wavelength observed in our Cu:$Zn_xCd_{1-x}S$ d-dots can undoubtedly rule out the possibility of excitonic emission, the peak position and broad nature of the claimed Cu dopant emission resemble the surface trap emission of the corresponding $Zn_xCd_{1-x}S$ host NCs. To determine whether it is Cu dopant emission or surface trap emission, we carried out the PL lifetime measurement. It has been reported that the intrinsic defects, size-dependent band gap, and surface defects of NCs are all involved in the PL emission.[57] Different electron−hole recombination mechanisms may correspond to different PL decay lifetimes. Normally, lifetime of the excitonic emission as well as the surface trap emission for various semiconductor NCs fall on the order of 1 and 10s of nanoseconds (ns), respectively,[58−61] whereas dopant emission in doped NCs, in which an additional energy state has been incorporated by dopant, is expected to have a longer excited-state lifetime. For example, the lifetimes of Cu dopant emission in Cu:ZnSe and Cu:ZnS/$Zn_xCd_{1-x}S$ d-dots have been reported on the order of 100s of ns,[43,44] and those for Mn emission in Mn:ZnSe and Mn:ZnS d-dots were 100s of μs.[27−29] We performed the measurement of the decay curves of the PL emission with representative emission wavelengths of 563, 633, and 698 nm from the Cu:$Zn_xCd_{1-x}S$ samples with corresponding Cd/Zn ratios of 1.2, 4.6, and 18.3, respectively. Herein, the room temperature PL decay time (i.e., the excited state lifetimes, $\tau_{1/e}$), at which the PL intensity has decreased to 1/e of its initial value, is used as a parameter to compare the lifetimes. We observed the PL excited-state lifetime located in the range of 100s of ns, and it enhanced with an increase of Cd ratio in the alloyed host NCs (Figure 4). This observed longer lifetime confirms the emission associated with Cu dopant transition but not from surface states of host NCs.

Effect of Reaction Temperature. A doping process actually includes multiple elementary (or quasielementary) steps, such as surface adsorption/desorption, lattice incorporation/ejection, and lattice diffusion, etc.[23] Each of which possesses its own critical reaction temperature. These distinguishable processes seem to be commonly present in different doping systems; therefore, selecting an advisible temperature is a key factor for the formation of high quality d-dots. In order to determine the best reaction temperature in the Cu:$Zn_xCd_{1-x}S$ d-dot system, UV−vis absorption and the PL emission spectra under different reaction temperature were

dx.doi.org/10.1021/ic2024023 | Inorg. Chem. 2012, 51, 3579−3587

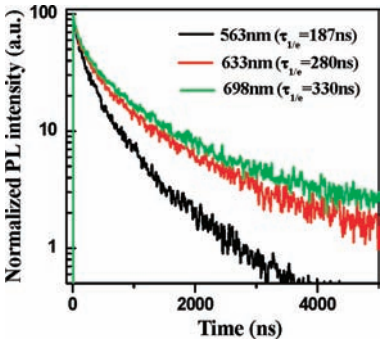

Figure 4. PL decay curves of Cu:$Zn_xCd_{1-x}S$ d-dots with representative emission wavelengths.

recorded. When the reaction temperature was higher than 80 °C, the Cu dopant PL emission gave rise and was increased slowly because of "lattice adsorption" of surface adsorbed Cu ions onto the surface lattice. If the dopant ions cannot incorporate into the host lattice and be reasonably isolated from the solution environment before it can act as an electron–hole recombination center, the dopant PL was very low and unstable. With an increase of the reaction temperature (from 80 to 200 °C), the dopant PL peak position red-shifted significantly and the PL intensity increased steadily as shown in Figure S2A. On the other hand, Figure S2B shows that the first excitonic absorption peak ascribed to the intrinsic $Zn_xCd_{1-x}S$ alloyed NCs became less pronounced and red-shifted (from 330 to 386 nm) gradually with the increase of reaction temperature. When the temperature was increased from 200 to 220 °C, a sharp increase of the dopant PL intensity was observed as shown in Figure 5A. The abrupt increase of PL

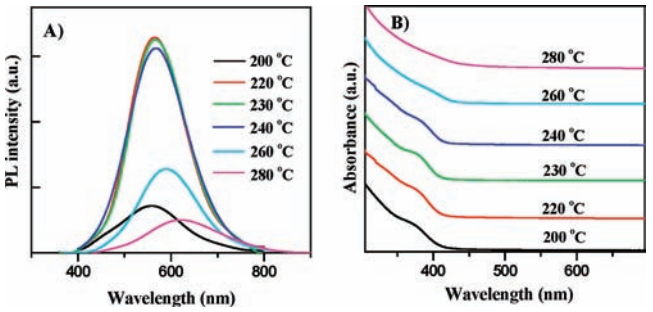

Figure 5. Evolution of (A) absorption and (B) PL emission spectra of Cu:$Zn_xCd_{1-x}S$ d-dots under growth temperatures from 200 to 280 °C with fixation of growth time of 30 min.

intensity was ascribed to the transition of "lattice adsorption" to the process of "lattice diffusion". It means that the critical temperature for lattice diffusion for Cu:$Zn_xCd_{1-x}S$ d-dots system would be about 205–215 °C. This indicates that this "lattice diffusion" step is an intrinsic step and could be decoupled from the "lattice adsorption" steps. After the sharp increase in PL intensity, the dopant PL became stable until the temperature reached about 240 °C and the first excitonic absorption peak position and shape in UV spectra did not change remarkably as shown in Figure 5B. Above 240 °C, the dopant PL intensity started to decrease, the peak position shifted to long wavelength furthermore, and the UV–vis absorption spectrum became featureless, which all indicated the occurrence of Ostwald ripening in this high temperature range. If the reaction temperature was too high (>280 °C), precipitation of the NCs within the reaction mixture occurred. The observed precipitation can be attributed to the fact that DDT acts as both the sulfur precursor and the stabilizing ligand during the reaction. Therefore, its gradual decomposition at too high a temperature results in a destabilization of the colloids.

Effect of Dopant Concentration. Several research groups have found that the PL QY of d-dots is dependent on the dopant concentration.[11,22,46,47] In order to study the influence of the Cu ions concentration on PL properties of Cu:$Zn_xCd_{1-x}S$ d-dots, a series of Cu:$Zn_xCd_{1-x}S$ d-dot samples with different nominal Cu/(Cd + Zn) ratios (from 0.5% to 10%) were prepared while keeping the other experimental variables fixed (i.e., gross amount of Cd and Zn at 0.2 mmol, Cd/Zn ratio of

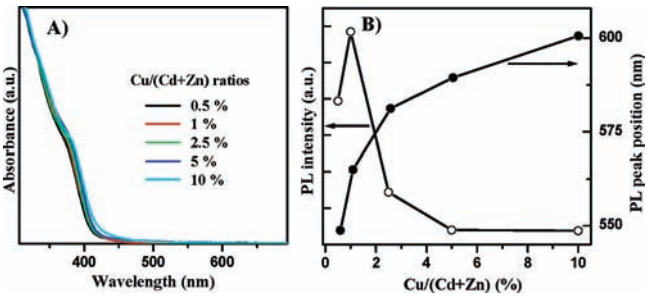

Figure 6. Evolution of (A) UV–vis absorption spectrum and (B) PL emission intensity and peak position under different Cu/(Cd + Zn) ratios (0.5–10%) with fixation of growth time of 30 min.

1:1, and reaction temperature of 220 °C). Figure 6A indicates that the absorption spectra of Cu:$Zn_xCd_{1-x}S$ d-dots in the presence of varying amounts of Cu show an almost identical spectra profile. The fixed position of the excitonic absorption peak indicates that the size and composition of the host alloyed NCs did not depend on the amount of dopant Cu added. Compared with the almost identical absorption spectra, the PL intensity and peak position in the PL emission spectra of the Cu:$Zn_xCd_{1-x}S$ d-dots show a remarkable dependence on the Cu precursor contents, and this dependence was summarized in Figure 6B. The PL emission peak shifted from 550 to 600 nm with increasing content of Cu, and the PL intensity showed a maximum value at about 1% Cu concentration. With the increase of Cu/(Cd + Zn) ratio (from 1% to 5%), the PL intensity decreased gradually and kept constant after the Cu/(Cd + Zn) ratios above 5%.

Overcoating Cu:$Zn_{1-x}Cd_xS$ NCs with ZnS Shell. For the case of binary or ternary semiconductor NC system such as CdSe, CdTe, and $CuInS_2$, or the transition metal doped semiconductor NCs such as Mn:ZnSe d-dots, the surface coating of nanoparticles with a higher band gap semiconductor, such as ZnS and CdS, has been reported to enhance PL QYs 4–10 times greater than those without coating,[29,49,52,62–65] due to both carrier confinement in the core and passivation of the surface recombination sites of the original particles. To improve the PL QY and stability of the Cu dopant emission in the obtained Cu:$Zn_xCd_{1-x}S$ d-dots, the Cu:$Zn_xCd_{1-x}S$/ZnS core/shell structure was constructed *in situ* from the crude Cu:$Zn_xCd_{1-x}S$ d-dot reaction solution. Due to the existence of excess of sulfur in the preparation of Cu:$Zn_xCd_{1-x}S$ d-dots, no additional sulfur source was added in the process of depositing ZnS shell. To avoid formation of separate ZnS nanoparticles, Zn precursor ($Zn(OAc)_2$) was added in portions (see details in

dx.doi.org/10.1021/ic2024023 | *Inorg. Chem.* 2012, 51, 3579–3587

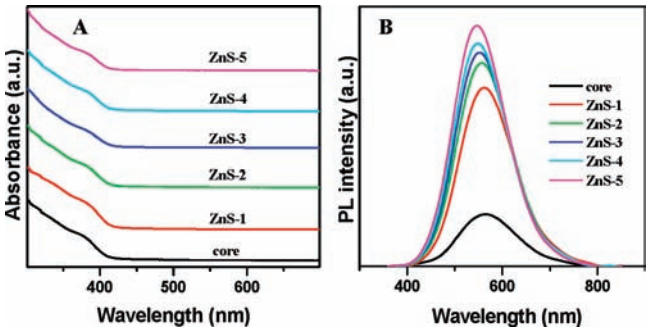

Figure 7. Evolution of (A) UV–vis absorption and (B, λ_{ex} = 350 nm) PL emission spectra of the resulting Cu:$Zn_{1-x}Cd_xS$/ZnS d-dots with deposition of different amount of ZnS shell around the core NCs.

the Experimental Section). Figure 7 shows the evolution of optical spectra of Cu:$Zn_xCd_{1-x}S$/ZnS core/shell NCs starting from the Cu:$Zn_xCd_{1-x}S$ cores under a nominal Zn:Cd ratio of 1:1. Growth of the ZnS shell improved the emission properties substantially, although it did not affect the absorption spectra significantly (Figure 7A). With the formation of Cu:$Zn_xCd_{1-x}S$/ZnS core/shell nanostructure, the PL peak position blue-shifted slightly from the original 565 to 546 nm, and the corresponding PL intensity increased about 10 times (Figure 7B). The blue shift of the PL peak position in the process of ZnS overcoating indicates further incorporation of the zinc component into the core material, resulting in an increase of the band gap energy. A similar result was also observed in the CuInS/ZnS and ZnCuInS/ZnS systems in previous literature.[49,52] Before deposition of ZnS shell, the Cu:$Zn_xCd_{1-x}S$ plain core NCs did show PL emission but with quite low PL QYs (typically below 6%). After ZnS shell growth, the PL properties of the resulting core/shell NCs became quite good. Without substantial optimization, the PL QY increased more than 10 times and the highest PL QY reached 65%. This QY is among the highest reported values for Cu d-dots to date,[37−47] and opens a way for the use of Cu:$Zn_xCd_{1-x}S$/ZnS NCs in many applications such as light-emitting devices or fluorescent biological labeling and sensing. To confirm that the enhancement of PL QY is due to overgrowth of ZnS shell but not to efficient Cu incorporation, we measured the Cu/Cd ratios before and after the ZnS shell deposition by ICP-AES. Experimental results show that the Cu/Cd ratios were kept almost constant before and after ZnS shell deposition (1:48.5, and 1:49.3, respectively). This result confirms our suggestion that the enhancement of dopant emission benefits from the deposition of ZnS shell around the Cu:$Zn_xCd_{1-x}S$ d-dots, but not from the efficient Cu incorporation.

The TEM image and XRD patterns for the representative Cu:$Zn_xCd_{1-x}S$/ZnS NCs starting from Cu:$Zn_xCd_{1-x}S$ core template with nominal Cd/Zn ratio of 1:1 are shown in Figure 2. A remarkable increase in particle size from approximately 3.2 to 4.5 nm can be observed upon shell growth. The obtained core/shell NCs contained roughly two monolayers of ZnS shell (the thickness of ZnS monolayer is taken as 0.6 nm). The samples of the representative Cu:$Zn_xCd_{1-x}S$/ZnS core/shell NCs have a narrow size distribution with a relative standard deviation (σ) of ~10% without any post-preparation fractionation or size sorting. The thin ZnS shell not only dramatically decreased the surface defects and increased the fluorescence efficiency but also offered a highly photostable structure. The XRD patterns of Cu:$Zn_xCd_{1-x}S$/ZnS preserved the zinc blende structure of the Cu:Zn$x$$Cd_{1-x}S$ core, but the diffraction peak shifted to the ZnS side furthermore due to the increase of ZnS content.

The evidence for the formation of the ZnS shell comes from the observation that, with the introduction of Zn precursor into the Cu:$Zn_xCd_{1-x}S$ crude reaction solution containing excess amount of sulfur precursor, the final particle size increased from the original 3.2 to 4.5 nm as indicated by TEM results. Optical spectral data confirm further the increased size derived from ZnS but not from $Zn_xCd_{1-x}S$. In the growth process of Cu:$Zn_xCd_{1-x}S$ core NCs, by extending the growth time from 30 to 120 min, the PL peak position is only shifted slightly from 565 to 574 nm (Figure 1B). This slight shift of PL peak position indicates that the Cu:$Zn_xCd_{1-x}S$ core size and composition have no remarkable change during this annealing process. While in the ZnS shell coating process under the same temperature (220 °C), the PL peak position is blue-shifted from the original 565 to 546 nm (Figure 7B). This blue-shift clearly demonstrates that the composition of the increased shell is ZnS but not $Zn_xCd_{1-x}S$; otherwise, a red-shift but not a blue-shift of the PL peak should be observed. Furthermore, the observed constant Cu/Cd ratio before and after ZnS shell deposition as discussed above also supports our conclusion that the composition of the shell is ZnS but not the $Zn_xCd_{1-x}S$ alloy; otherwise, the measured Cu/Cd ratio should decrease. Due to the atomic diffusion, there is no clear interface between the Cu:$Zn_xCd_{1-x}S$ core and ZnS shell. On the other hand, due to the similar lattice parameter of ZnS and $Zn_xCd_{1-x}S$, it is almost impossible to distinguish the ZnS shell and Cu:$Zn_xCd_{1-x}S$ core in the TEM.

In this studied core/shell structure, since the band gap of host $Zn_xCd_{1-x}S$ alloyed NCs can be conveniently tuned via variation of the Cd/Zn ratio, the dopant emission wavelength of the resulting Cu:$Zn_{1-x}Cd_xS$/ZnS core/shell structure can also be tuned through variation of the Cd/Zn ratio in the starting Cu:$Zn_xCd_{1-x}S$ core NCs. The UV–vis spectra (Figure 8A) indicate that the band edge of the NCs moved along with the tuning of the emission. As shown in Figure 8B, the emission wavelength of the Cu:$Zn_xCd_{1-x}S$/ZnS NCs starting from

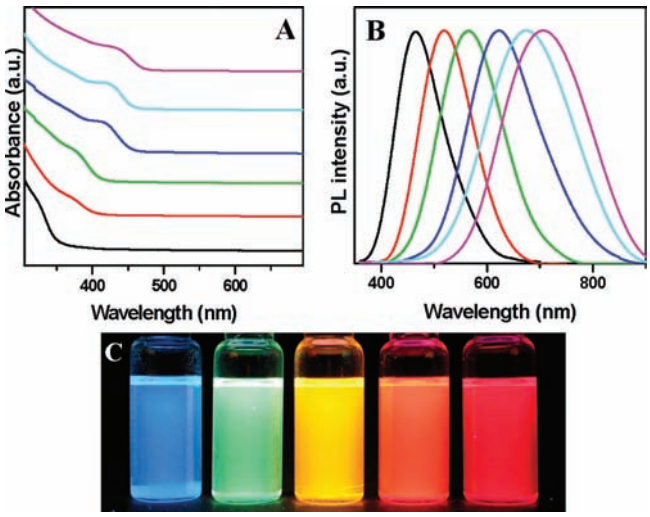

Figure 8. Normalized (A) UV–vis absorption and (B, λ_{ex} = 350 nm) corresponding PL emission spectra of Cu:$Zn_xCd_{1-x}S$/ZnS d-dots under different Cd/Zn precursor ratios. (C) Digital picture of samples under the radiation of a UV lamp.

dx.doi.org/10.1021/ic2024023 | Inorg. Chem. 2012, 51, 3579–3587

Cu:$Zn_xCd_{1-x}S$ core NCs with different Cd/Zn ratios can cover the entire visible spectrum and partial near-infrared window (from 440 to 710 nm) with high brightness. A digital picture of the Cu:$Zn_xCd_{1-x}S$/ZnS samples under UV excitation is shown in Figure 8C. The best PL QY of the dopant emission has been observed to be 65%, and the average value is in the range 45−55%. The obtained Cu dopant emission can span the entire visible spectral window and could be a potential color tunable dispersed NC emitter with applications such as light-emitting devices, lasers, and biomedical fluorescent labels.

Stable Water-Soluble d-Dots. The as-prepared Cu:$Zn_xCd_{1-x}S$/ZnS d-dots not only show high PL QYs in the organic media but also retain high luminescent brightness when transferred into aqueous media via ligand replacement by MUA. Our experimental results show that the water-soluble Cu:$Zn_xCd_{1-x}S$/ZnS d-dots can keep up to 75% of the luminescent intensity of the initial oil-soluble NCs (Figure 9A). For visibility, Figure 9B shows the luminescence photographs of two representative Cu:$Zn_xCd_{1-x}S$/ZnS d-dots with an emission wavelength in the visible light range to demonstrate the highly bright luminescence in both oil media and aqueous media under illumination by a UV lamp. The high luminescence of Cu:$Zn_xCd_{1-x}S$/ZnS d-dots in aqueous media can be retained for several days without observable quenching. This high PL stability of the water-soluble QDs renders them of special interest in the in vivo imaging application.

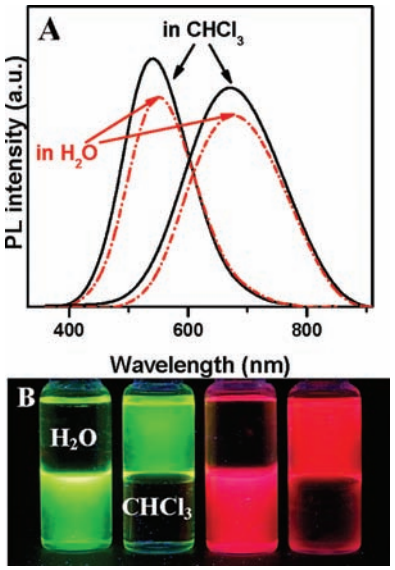

Figure 9. (A) PL spectra of Cu:$Zn_xCd_{1-x}S$/ZnS samples before (toluene solutions) and after (aqueous solutions) phase transfer using MUA. All colloidal solutions exhibit identical optical densities at the excitation wavelength. (B) Photographs of samples dispersed in different media under illumination of a UV lamp.

Thermal Stability. As reported above, the emission for the Cu dopant is associated with the Cu atomic level, and therefore, it should thus be less coupled with lattice vibration in comparison to the excitonic of undoped semiconductor NCs.[42] Visually, these Cu-doped alloyed NCs did not show a significant change in luminescence brightness upon heating to 250 °C (Figure 10), whereas generally undoped quantum dots suffer almost complete quenching of its band gap PL at about 150 °C.[42] When the sample was cooled to room temperature, the emission intensity was almost recovered. The results of the observed thermal-stability feature of the PL further confirmed that the emission of the d-dots originated from the doping centers but not from the trap emission. The outstanding thermal stability of the dopant PL from Cu:$Zn_xCd_{1-x}S$/ZnS d-dots further solidifies their many applications such as light-emitting devices or fluorescent biological labeling and sensing.

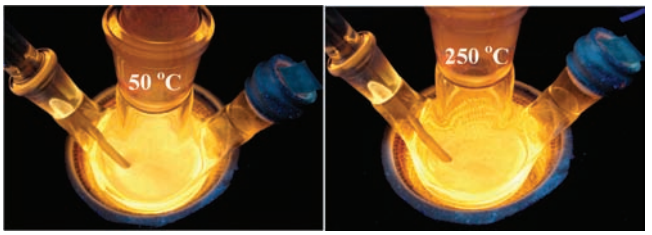

Figure 10. PL images of Cu:$Zn_xCd_{1-x}S$/ZnS d-dots under different temperatures.

CONCLUSIONS

For the first time, Cu:$Zn_xCd_{1-x}S$/ZnS d-dots with tunable PL emission covering the entire visible spectrum and high PL QYs in the range 50−65% have been prepared via a facile noninjection and low cost approach using CdO, $Zn(OAc)_2$, $Cu(OAc)_2$, and elemental sulfur as precursors. The Cu dopant emission wavelength in the host alloyed NCs can be conveniently tuned via variation of the stoichiometric ratio of their components. The experimental variables, including the Cd/Zn ratio, amount of dopant, and reaction temperature, have a significant effect on the Cu dopant emission of the obtained d-dots, and this tunable dopant emission covers the entire visible spectral window (from 440 to 710 nm). The Cu:$Zn_xCd_{1-x}S$ d-dots did show PL emission but with a quite low PL QY (typically below 6%). With the deposition of ZnS shell around the Cu:$Zn_xCd_{1-x}S$ core NCs, the PL QY increased substantially with a maximum value of 65%. These obtained d-dots also retain high PL QY when transferred into aqueous media via ligand replacement by MUA. In addition, these d-dots have thermal stability (stable up to 250 °C), and a long PL decay lifetime (100s of nanoseconds). These outstanding properties render the Cu:$Zn_xCd_{1-x}S$/ZnS d-dots for promising applications such as light-emitting devices, lasers, and biomedical fluorescent labels. Furthermore, this reported facile noninjection strategy provides a versatile route to large-scale preparation of other doped semiconductor NCs.

ASSOCIATED CONTENT

Supporting Information

TEM images of Cu:$Zn_xCd_{1-x}S$ d-dots upon different Cd/Zn precursor ratios, and PL emission and UV−vis absorption spectra of Cu:$Zn_xCd_{1-x}S$ d-dots under different reaction temperatures. This material is available free of charge via the Internet at http://pubs.acs.org.

AUTHOR INFORMATION

Corresponding Author

*E-mail: zhongxh@ecust.edu.cn. Fax: +86 21 6425 0281.

Notes

The authors declare no competing financial interest.

ACKNOWLEDGMENTS

We thank the National Natural Science Foundation of China (21175043), the Science and Technology Commission of

Shanghai Municipality (11JC1403100), State Key Laboratory of Chemical Engineering (SKL-ChE-09C01), the Fundamental Research Funds for the Central Universities, and the Program for Professor of Special Appointment at Shanghai Institutions of Higher Learning for financial support.

REFERENCES

(1) (a) Urban, J. J.; Talapin, D. V.; Shevchenko, E. V.; Kagan, C. R.; Murray, C. B. *Nat. Mater.* **2007**, *6*, 115−121. (b) Rogach, A. L.; Gaponik, N.; Lupton, J. M.; Bertoni, C.; Gallardo, D. E.; Dunn, S.; Pira, N. L.; Paderi, M.; Repetto, P.; Romanov, S. G.; O'Dwyer, C.; Torres, C. M. S.; Eychmuller, A. *Angew. Chem., Int. Ed.* **2008**, *35*, 6538−6549.
(2) Gur, I.; Fromer, N. A.; Geier, M. L.; Alivisatos, A. P. *Science* **2005**, *310*, 462−465.
(3) Konstantatos, G.; Howard, I.; Fischer, A.; Hoogland, S.; Clifford, J.; Klem, E.; Levina, L.; Sargent, E. H. *Naure* **2006**, *442*, 180−183.
(4) Nozik, A. J.; Beard, M. C.; Luther, J. M.; Law, M.; Ellingson, R. J.; Johnson, J. C. *Chem. Rev.* **2010**, *110*, 6873−6890.
(5) Yang, Z. S.; Chen, C. Y.; Roy, P.; Chang, H. T. *Chem. Commun.* **2011**, *47*, 9561−9571.
(6) Li, L.; Yang, X. C.; Gao, J. J.; Tian, H. N.; Zhao, J. Z.; Hagfeldt, A.; Sun, L. C. *J. Am. Chem. Soc.* **2011**, *133*, 8458−8460.
(7) Somers, R. C.; Bawendi, M. G.; Nocera, D. G. *Chem. Soc. Rev.* **2007**, *36*, 579−591.
(8) (a) Zrazhevskiy, P.; Sena, M.; Gao, X. H. *Chem. Soc. Rev.* **2010**, *39*, 4326−4354. (b) Li, Y.; Jing, L.; Qiao, R.; Gao, M. *Chem. Commun.* **2011**, *33*, 9293−9311.
(9) Delehanty, J. B.; Bradburne, C. E.; Susumu, K.; Boeneman, K.; Mei, B. C.; Farrell, D.; Blanco-Canosa, J. B.; Dawson, P. E.; Mattoussi, H.; Medintz, I. L. *J. Am. Chem. Soc.* **2011**, *133*, 10482−10489.
(10) Peng, X. *Acc. Chem. Res.* **2010**, *43*, 1387−1395.
(11) Norris, D. J.; Efros, A. L.; Erwin, S. C. *Science* **2008**, *319*, 1776−1779.
(12) Erwin, S. C.; Zu, L.; Haftel, M. I.; Efros, A. L.; Kennedy, T. A.; Norris, D. J. *Nature* **2005**, *436*, 91−94.
(13) (a) Suyver, J. F.; Wuister, S. F.; Kelly, J. J.; Meijerink, A. *Nano Lett.* **2001**, *1*, 429. (b) Bol, A. A.; Meijerink, A. *J. Phys. Chem. B* **2001**, *105*, 10197. (c) Suyver, J. F.; Wuister, S. F.; Kelly, J. J.; Meijerink, A. *Phys. Chem. Chem. Phys.* **2000**, *2*, 5445.
(14) Hanif, K. M.; Meulenberg, R. W.; Strouse, G. F. *J. Am. Chem. Soc.* **2002**, *124*, 11495−11502.
(15) Norberg, N. S.; Kittilstved, K. R.; Amonette, J. E.; Kukkadapu, R. K.; Schwartz, D. A.; Gamelin, D. R. *J. Am. Chem. Soc.* **2004**, *126*, 9387−9398.
(16) Norris, D. J.; Yao, N.; Charnock, F. T.; Kennedy, T. A. *Nano Lett.* **2001**, *1*, 3−7.
(17) Pradhan, N.; Goorskey, D.; Thessing, J.; Peng, X. *J. Am. Chem. Soc.* **2005**, *127*, 17586−17587.
(18) Yang, Y.; Chen, O.; Angerhofer, A.; Cao, Y. C. *J. Am. Chem. Soc.* **2006**, *128*, 12428−12429.
(19) Pradhan, N.; Peng, X. *J. Am. Chem. Soc.* **2007**, *129*, 3339−3347.
(20) Pradhan, N.; Battaglia, D. M.; Liu, Y. C.; Peng, X. G. *Nano Lett.* **2007**, *7*, 312−317.
(21) Yang, Y.; Chen, O.; Angerhofer, A.; Cao, Y. C. *J. Am. Chem. Soc.* **2008**, *130*, 15649−15661.
(22) Nag, A.; Chakraborty, S.; Sarma, D. D. *J. Am. Chem. Soc.* **2008**, *130*, 10605−10611.
(23) Chen, D.; Viswanatha, R.; Ong, G. L.; Xie, R.; Balasubramaninan, M.; Peng, X. *J. Am. Chem. Soc.* **2009**, *131*, 9333−9339.
(24) Wood, V.; Halpert, J. E.; Panzer, M. J.; Bawendi, M. G.; Bulovic, V. *Nano Lett.* **2009**, *9*, 2367−2371.
(25) Quan, Z.; Yang, D.; Li, C.; Kong, D.; Yang, P.; Cheng, Z.; Lin, J. *Langmuir* **2009**, *25*, 10259−10262.
(26) Wang, C.; Gao, X.; Ma, Q.; Xu, X. *J. Mater. Chem.* **2009**, *19*, 7016−7022.
(27) Zheng, J.; Yuan, X.; Ikezawa, M.; Jing, P.; Liu, X.; Zheng, Z.; Kong, X.; Zhao, J.; Masumoto, Y. *J. Phys. Chem. C* **2009**, *113*, 16969−16974.
(28) Zheng, J.; Ji, W.; Wang, X.; Ikezawa, M.; Jing, P.; Liu, X.; Li, H.; Zhao, J.; Masumoto, Y. *J. Phys. Chem. C* **2010**, *114*, 15331−15336.
(29) Fang, Z.; Wu, P.; Zhong, X.; Yang, Y. J. *Nanotechnology* **2010**, *21*, 305604.
(30) Zeng, R.; Rutherford, M.; Xie, R.; Zou, B.; Peng, X. *Chem. Mater.* **2010**, *22*, 2107−2113.
(31) Srivastava, B. B.; Jana, S.; Karan, N. S.; Paria, S.; Jana, N. R.; Sarma, D. D.; Pradhan, N. *J. Phys. Chem. Lett.* **2010**, *1*, 1454−1458.
(32) Acharya, S.; Sarma, D. D.; Jana, N. R.; Pradhan, N. *J. Phys. Chem. Lett.* **2010**, *1*, 485−488.
(33) Zhu, D.; Jiang, X.; Zhao, C.; Sun, X.; Zhang, J.; Zhu., J. *Chem. Commun.* **2010**, *46*, 5226−5228.
(34) Zeng, R.; Zhang, T.; Dai, G.; Zou., B. *J. Phys. Chem. C* **2011**, *115*, 3005−3010.
(35) Deng, Z.; Tong, L.; Flores, M.; Liu, S.; Cheng, J. -X.; Yan, H.; Liu, Y. *J. Am. Chem. Soc.* **2011**, *131*, 5388−5389.
(36) Zhang, W.; Li, Y.; Zhang, H.; Zhou, X.; Zhong, X. *Inorg. Chem.* **2011**, *50*, 10432−10438.
(37) Sun, L.; Liu, C.; Liao, C.; Yan., C. *J. Mater. Chem.* **1999**, *9*, 1655−1657.
(38) Meulenberg, R. W.; Buuren, T. V.; Khalid., M.; Willey, T. M.; Strouse, G. F.; Terminello, L. J. *Nano Lett.* **2004**, *4*, 2277−2285.
(39) Ehlert, O.; Osvet, A.; Batentschuk, M.; Winnacker, A.; Nann, T. *J. Phys. Chem. B* **2006**, *110*, 23175−23178.
(40) Corrado, C.; Hawker, M.; Livingston, G.; Medling, S.; Bridges, F.; Zhang, J. *Nanoscale* **2010**, *2*, 1213−1221.
(41) (a) Datta, A.; Biswas, S.; Kar, S.; Chaudhuri, S. *J. Nanosci. Nanotechnol.* **2007**, *7*, 3670−3676. (b) Chien, N. D.; Chung, H. V.; Huy, P. T.; Kim., D.; Ferrari, M. *Adv. Mater. Res.* **2008**, *31*, 114−116.
(42) Xie, R.; Peng, X. *J. Am. Chem. Soc.* **2009**, *131*, 10645−10651.
(43) Jana, S.; Srivastava, B. B.; Acharya, S.; Santra, P. K.; Jana, N. R.; Sarma, D. D.; Pradhan, N. *Chem. Commun.* **2010**, *46*, 2853−2855.
(44) Srivastava, B. B.; Jana, S.; Pradhan, N. *J. Am. Chem. Soc.* **2011**, *133*, 1007−1015.
(45) Sarkar, S.; Karan, N. S.; Pradhan, N. *Angew. Chem., Int. Ed.* **2011**, *50*, 6065−6069.
(46) Shen, H.; Wang, H.; Li, X.; Niu, J.; Wang, H.; Chen, X.; Li, L. *Dalton Trans.* **2009**, 10534−10540.
(47) Karan, N. S.; Sarma, D. D.; Kadam, R. M.; Pradhan, N. *J. Phys. Chem. Lett.* **2010**, *1*, 2863−2866.
(48) (a) Peka, P.; Schulz, H. J. *Physica B* **1994**, *193*, 57−65. (b) Corrado, C.; Jiang, Y.; Oba, F.; Kozina, M.; Bridges, F.; Zhang, J. Z. *J. Phys. Chem. A* **2009**, *113*, 3830−3839. (c) Mandal, P.; Talwar, S. S.; Major, S. S.; Srinivasa, R. S. *J. Chem. Phys.* **2008**, *128*, 114703/1−114703/7. (d) Stouwdam, J. W.; Janssen, R. A. J. *Adv. Mater.* **2009**, *21*, 2916−2920.
(49) Zhang, W.; Zhong, X. *Inorg. Chem.* **2011**, *50*, 4065−4072.
(50) Zhong, X.; Han, M.; Dong, Z.; White, T. J.; Knoll, W. *J. Am. Chem. Soc.* **2003**, *125*, 8589−8594.
(51) Zhong, X.; Feng, Y.; Knoll, W.; Han, M. *J. Am. Chem. Soc.* **2003**, *125*, 13559−13563.
(52) Xie, R.; Rutherford, M.; Peng, X. *J. Am. Chem. Soc.* **2009**, *131*, 5691−5697.
(53) Kruszynska, M.; Borchert, H.; Parisi, J.; Kolny-Olesiak, J. *J. Am. Chem. Soc.* **2010**, *132*, 15976−15982.
(54) Greenham, N. C.; Peng, X.; Alivisatos, A. P. *Phys. Rev. B* **1996**, *54*, 17628−17637.
(55) Zhong, X.; Liu, S.; Zhang, Z.; Li, L.; Wei, Z.; Knoll, W. *J. Mater. Chem.* **2004**, *14*, 2790−2794.
(56) Kamat, P. V. *J. Phys. Chem. C* **2008**, *112*, 18737−18753.
(57) Zhang, J. Z. *Acc. Chem. Res.* **1997**, *30*, 423−429.
(58) Sapra, S.; Prakash, A.; Ghangrekar, A.; Periasamy, N.; Sarma, D. D. *J. Phys. Chem. B* **2005**, *109*, 1663−1668.
(59) Chamarro, M. A.; Voliotis, V.; Grousson, R.; Lavallard, P.; Gacoin, T.; Counio, G.; Boilot, J. P.; Cases, R. *J. Cryst. Growth.* **1996**, *159*, 853−856.

(60) Califano, M.; Franceschetti, A.; Zunger, A. *Nano Lett.* **2005**, *5*, 2360−2364.
(61) Zhang, J.; Zhang, X.; Zhang, J. Y. *J. Phys. Chem. C* **2009**, *113*, 9512−9515.
(62) Talapin, D. V.; Mekis, I.; Gotzinger, S.; Kornowski, A.; Benson, O.; Weller, H. *J. Phys. Chem. B* **2004**, *108*, 18826−18831.
(63) Zhang, W.; Chen, G.; Wang, J.; Ye, B.; Zhong, X. *Inorg. Chem.* **2009**, *48*, 9723−9731.
(64) Li, L.; Daou, T. J.; Texier, I.; Chi, T. T. K.; Liem, N. Q.; Reiss, P. *Chem. Mater.* **2009**, *21*, 2422−2429.
(65) Talapin, D. V.; Koeppe, R.; Gotzinger, S.; Kornowski, A.; Lupton, J. M.; Rogach, A. L.; Benson, O.; Feldmann, J.; Weller, H. *Nano Lett.* **2003**, *3*, 1677−1681.